

**INVESTIGATION ON VERSATILE CASCADE
LATENT HEAT STORAGE SYSTEM FOR
SOLAR COOKING APPLICATIONS**

SHUBHAM JAIN



**DEPARTMENT OF ENERGY SCIENCE AND ENGINEERING
INDIAN INSTITUTE OF TECHNOLOGY DELHI**

JANUARY 2025

© Indian Institute of Technology Delhi (IITD), New Delhi, 2025

**INVESTIGATION ON VERSATILE CASCADE
LATENT HEAT STORAGE SYSTEM FOR
SOLAR COOKING APPLICATIONS**

by

SHUBHAM JAIN

Department of Energy Science and Engineering

submitted

**in fulfillment of the requirements of the degree of Doctor of Philosophy
to the**



INDIAN INSTITUTE OF TECHNOLOGY DELHI

January 2025

Certificate

This is to certify that the thesis entitled "**Investigation on Versatile Cascade Latent Heat Storage System for Solar Cooking Applications**" being submitted by **Mr. Shubham Jain** (Entry Number: 2019ESZ8272) to the Indian Institute of Technology Delhi in fulfillment of the requirements for the award of the degree of **Doctor of Philosophy** is a record of bonafide research work performed by him under our guidance and supervision at **Department of Energy Science and Engineering, Indian Institute of Technology Delhi, India.**

The results obtained herein have not been submitted in part or in full to any other University or Institute for the award of any degree to the best of my knowledge.



Dr. K. Ravi Kumar
Associate Professor,
Department of Energy Science and Engineering,
Indian Institute of Technology Delhi, India



Prof. Dibakar Rakshit
Professor,
Department of Energy Science and Engineering,
Indian Institute of Technology Delhi, India

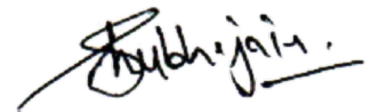
Acknowledgments

I am deeply pleased to express my heartfelt gratitude to all those who supported me throughout my journey during my doctoral study. First and foremost, I extend my sincere thanks and profound appreciation to my Ph.D. advisors, Prof. K. Ravi Kumar and Prof. Dibakar Rakshit, for their invaluable guidance, thoughtful insights, and unwavering support during my Ph.D. studies at the Department of Energy Science and Engineering, Indian Institute of Technology Delhi. Their encouragement has been a constant source of inspiration since I embarked on this exciting research path.

I am also grateful to my research committee members, Prof. K. A. Subramanian, Prof. B. Premachandran, and Prof. Kaushik Saha. Their insightful feedback and invaluable advice during the various stages of my research evaluations have been crucial to the success of my work. I also want to thank the Head of the Department of Energy Science and Engineering for providing the necessary facilities and continuous support. I would like to extend my sincere gratitude to Prof. K. S. Reddy for his expert guidance and invaluable contributions throughout the development of the experimental test facilities, which were instrumental to the success of my research work. I would like to acknowledge the Department of Science and Technology (DST), Government of India, for funding this research through Project Number: DST/TMD/CERI/RES/2020/14(G). I am deeply thankful to Dr. Anish Malan, Dr. Ram Kumar Pal, Mr. Sumeet Kumar Dubey, Mr. Alok Kumar Ray, Mr. Rajeev Awasthi, Mr. Naveen T. K., Mr. Shantanu Kumar, Mr. Swamy Mallayya, Mr. Tarun Goyal, Mr. Shubhadeep Paul, Mr. Gaurav Arora, Mr. Ikhtedar Hussain Rizvi, Mr. Rahul Sharma and all my lab mates for their valuable suggestions, continuous encouragement, and generous assistance throughout my research.

Special thanks to my friend, Mr. Abhishek Kandpal, for his support and motivation during my doctoral journey. His encouragement has been instrumental in keeping me focused and inspired throughout this process. Additionally, I wish to extend my gratitude to the institute's administrative and technical staff. Their support and assistance have been invaluable throughout my doctoral program, and I deeply appreciate their efforts.

I profoundly thank my parents and sister for their unwavering support and blessings. My parents have been my pillars of strength throughout this journey, always motivating and encouraging me to achieve my best. Finally, my deepest gratitude goes to my wife, Mrs. Siksha Jain, for her unwavering love, support, and understanding throughout this research journey. Her encouragement, belief in my abilities, and the sacrifices she made have been a source of immense strength, enabling me to focus on my academic pursuits.

A handwritten signature in black ink, appearing to read 'Shubham Jain', with a horizontal line underneath.

(Shubham Jain)

Abstract

Food is vital for human existence, supplying the energy and nutrients for daily activities and overall health. A significant proportion of the global population relies on polluting fuels (firewood, animal dung, and agriculture waste) for daily cooking energy needs, which causes household air pollution. Adoption of clean cooking fuels (Liquified petroleum gas, natural gas, biogas, electricity, and solar) is necessary to prevent health hazards (respiratory and cardiovascular diseases) due to household air pollution. Moreover, the depletion of fossil fuel reserves and geopolitical instabilities are significantly increasing the cost of cooking fuels in developing countries. Utilization of solar energy (clean energy) for daily cooking applications can address these challenges appropriately. Solar energy can be utilized for cooking in the form of heat (from solar thermal collectors) or in the form of electricity (from solar photo-voltaic collectors). Although solar energy is abundantly present on Earth, its intermittency (diurnal and seasonal) and nocturnal unavailability create a considerable hindrance in its adoption for cooking applications. Furthermore, operational challenges, restrictions on food types, and the inability to prepare any kind of meal at any time of the day, regardless of weather conditions, pose significant technological barriers to the widespread adoption of existing community-scale indoor solar cooking systems. The integration of a suitable energy storage system, along with design modifications in existing cooking systems, is essential to increase the acceptability of solar cooking systems among people. Storing solar energy in thermal energy storage is more feasible than storing it in an electrochemical battery in terms of efficiency, operational simplicity, life cycle, economics, and ecological footprints. Therefore, collecting solar energy using solar thermal collectors and storing it in a thermal energy storage system for off-sun cooking applications is a viable option.

Latent heat storage technology excels among other technologies, such as sensible and thermochemical energy storage, owing to its high energy density, operational simplicity,

environmental feasibility, easy availability, and cost-effectiveness. Latent heat storage stores thermal energy as phase transition enthalpy of phase change materials. The poor thermal conductivity of phase change materials significantly affects the thermal performance of the latent heat storage systems. This highlights the need to incorporate heat transfer augmentation techniques during their integration in any application.

The necessity of the present work originates from the paucity of studies exploring the possibility of developing a latent heat storage technology for supporting multi-temperature-based indoor solar cooking applications. Various food items require different temperatures during cooking, i.e., baking, frying, and boiling, which require an end-use temperature of 453-493 K, 383-443 K, and 373-393 K, respectively. The foundation of the design of the latent heat storage system is laid on a few requisites, i.e., storage should be compact, cost-effective, efficient, should have a faster charging rate (it is necessary while coupling the storage with solar thermal collectors due to diurnal variation of solar radiation), should require less maintenance, and can maintain a stable supply of thermal energy at different temperatures. The research is initiated with the comparative assessment of single and multiple-phase change material-based storage systems using the enthalpy porosity technique-based numerical approach. It has been observed that in comparison to single-phase change material-based storage using NaNO_3 and NaNO_2 , a two-stage cascade latent heat storage system incorporating both phase change materials reduces the charging time by 35.23% and 10.52%, respectively. The cascade latent heat storage system maintains an augmented heat transfer rate between the heat transfer fluid and phase change materials during charging. It can also facilitate end-use applications at different temperatures.

Furthermore, numerical investigations are performed to find the simple, passive, economical, heat transfer augmentation methods for the cascade latent heat storage systems that are feasible for their commercial implementation. In this context, the effect of modification

of the shell, change of orientation of the storage, and eccentric repositioning of the heat transfer fluid passage on the thermal behavior of the shell and tube-based latent heat storage system are investigated. Changing the cylindrical shell to frustum in the latent heat storage system reduces the charging time by 18.42%. However, it adversely impacts the charging performance of the cascade latent heat storage system. The horizontal cylindrical cascade storage completes the charging in 39.04%, 15.78%, 24.70%, and 5.9%, respectively, less charging time than the other storage configurations, i.e., single-stage NaNO_3 storage, single-stage NaNO_2 storage, vertical frustum cascade storage, and vertical cylindrical cascade storage.

Based on the design guidelines that originated from the numerical investigations, a state-of-the-art versatile cascade latent heat storage system is developed. Furthermore, three innovatively designed cooking units, i.e., cooking plate, frying pan, and cooking vessel, are developed for baking, frying, and boiling-related cooking operations and integrated with the developed storage. This work thoroughly discusses the real-time cyclic (charging and discharging) thermal behavior of cascade storage, along with its capabilities to support different temperature-based end-use applications. The developed cascade latent heat storage system maintains the stable end-use temperature of 473 K, 452 K, and 373 K, respectively, at the cooking plate, frying pan, and cooking vessel for baking, frying, and boiling food products. Cooking time for baking a chapati (60 g), frying potato chips (80 g), and boiling potatoes (500 g) is observed as 4 minutes, 4 minutes, and 13 minutes, respectively. The cyclic and end-use efficiency of the cascade storage are obtained as 55.82% and 38.24%, respectively. The recommendations of the present research work will pave the way for the commercial establishment of cascade latent heat storage technology for multi-temperature-based solar thermal and industrial applications.

सारांश

भोजन मानव अस्तित्व के लिए अत्यंत आवश्यक है, क्योंकि यह दैनिक गतिविधियों और समग्र स्वास्थ्य के लिए ऊर्जा और पोषक तत्व प्रदान करता है। वैश्विक जनसंख्या का एक बड़ा हिस्सा अपनी दैनिक खाना पकाने की ऊर्जा आवश्यकताओं के लिए प्रदूषणकारी ईंधन (जैसे लकड़ी, गोबर, और कृषि अपशिष्ट) पर निर्भर है, जिससे घर के अंदर वायु प्रदूषण होता है। घर के अंदर वायु प्रदूषण के कारण स्वास्थ्य पर पड़ने वाले खतरों (जैसे श्वसन और हृदय रोग) को रोकने के लिए स्वच्छ ईंधन (जैसे एलपीजी, प्राकृतिक गैस, बायोगैस, बिजली, और सौर ऊर्जा) अपनाना आवश्यक है। इसके अलावा, जीवाश्म ईंधनों के भंडार की कमी और भू-राजनीतिक अस्थिरता विकासशील देशों में खाना पकाने के ईंधन की लागत में वृद्धि कर रही है। दैनिक खाना पकाने के लिए सौर ऊर्जा (स्वच्छ ऊर्जा) का उपयोग इन चुनौतियों को प्रभावी रूप से हल कर सकता है। सौर ऊर्जा का उपयोग खाना पकाने के लिए या तो ऊष्मा (सौर तापीय संग्रहकों से) के रूप में या बिजली (सौर फोटोवोल्टिक संग्रहकों से) के रूप में किया जा सकता है। हालाँकि पृथ्वी पर सौर ऊर्जा प्रचुर मात्रा में उपलब्ध है, इसकी अनियमितता (दैनिक और मौसमी) और रात में अनुपलब्धता इसे खाना पकाने के लिए अपनाने में बड़ी बाधा उत्पन्न करती है। इसके अतिरिक्त, परिचालन संबंधी चुनौतियाँ, भोजन प्रकारों पर परिसीमन, और मौसम की परवाह किए बिना किसी भी समय भोजन तैयार करने में असमर्थता, मौजूदा सामुदायिक-स्तरीय अन्तर गृहीय सौर खाना पकाने के निकाय की व्यापक स्वीकार्यता में बड़ी तकनीकी बाधाएँ हैं। मौजूदा खाना पकाने के निकाय में संरचना संशोधनों के साथ-साथ एक उपयुक्त ऊर्जा भंडारण प्रणाली का एकीकरण, सौर खाना पकाने के निकायों की लोगों के बीच स्वीकार्यता बढ़ाने के लिए आवश्यक है। सौर ऊर्जा को ऊष्मीय ऊर्जा भंडारण में संग्रहित करना, विद्युत रासायनिक बैटरी में संग्रहित करने की तुलना में दक्षता, संचालन में सरलता, जीवन चक्र, अर्थशास्त्र और पर्यावरणीय प्रभाव के मामले में अधिक व्यवहारिक है। इसलिए, सौर तापीय संग्रहकों का उपयोग करके

सौर ऊर्जा को इकट्ठा करना और इसे तापीय ऊर्जा भंडारण प्रणाली में सूरज की अनुपस्थिति में खाना पकाने के अनुप्रयोगों के लिए संग्रहित करना एक व्यावहारिक विकल्प है।

गुप्त ऊष्मा भंडारण तकनीक अन्य तकनीकों, जैसे संवेदनशील और ऊष्मा-रासायनिक ऊर्जा भंडारण, की तुलना में उच्च ऊर्जा घनत्व, संचालन में सरलता, पर्यावरणीय अनुकूलता, सुगम उपलब्धता और लागत प्रभावशीलता के कारण उत्कृष्ट है। गुप्त ऊष्मा भंडारण, फेज़ चेंज मटेरियल्स के अवस्था परिवर्तन एन्थैल्पी के रूप में ऊष्मा को संग्रहित करता है। फेज़ चेंज मटेरियल्स की खराब ऊष्मीय चालकता गुप्त ऊष्मा भंडारण प्रणाली के ऊष्मीय प्रदर्शन को काफी प्रभावित करती है। यह किसी भी अनुप्रयोग में उनके एकीकरण के दौरान ऊष्मा संचरण वृद्धि तकनीकों को शामिल करने की आवश्यकता को उजागर करता है।

इस कार्य की आवश्यकता इस तथ्य से उत्पन्न होती है कि गुप्त ऊष्मा भंडारण तकनीक को बहु-तापमान आधारित अंतर-गृहीय सौर खाना पकाने के अनुप्रयोगों का समर्थन करने के लिए विकसित करने की संभावना का पता लगाने वाले अध्ययनों की कमी है। विभिन्न खाद्य पदार्थों को पकाने के दौरान अलग-अलग तापमान की आवश्यकता होती है, जैसे सेंकने, तलने, और उबालने के लिए क्रमशः 453-493 K, 383-443 K, और 373-393 K का अंतिम उपयोग तापमान चाहिए। गुप्त ऊष्मा भंडारण प्रणाली की संरचना कुछ आवश्यकताओं पर आधारित है, जैसे कि यह संकुचित, किफायती, कुशल होना चाहिए, चार्जिंग की तीव्र दर (सौर तापीय संग्रहकों के साथ एकीकरण के दौरान सौर विकिरण के दैनिक परिवर्तन के कारण आवश्यक) होनी चाहिए, न्यूनतम रखरखाव की आवश्यकता होनी चाहिए, और विभिन्न तापमानों पर स्थिर ऊष्मीय ऊर्जा आपूर्ति बनाए रखनी चाहिए। अनुसंधान की शुरुआत एकल और बहु-फेज़ चेंज मटेरियल-आधारित भंडारण प्रणालियों के तुलनात्मक आंकलन से की गई, जिसमें एन्थैल्पी पोरोसिटी तकनीक-आधारित संख्यात्मक दृष्टिकोण का उपयोग किया गया। यह देखा गया कि NaNO_3 और NaNO_2 का उपयोग करने वाले एकल-फेज़ चेंज मटेरियल आधारित भंडारण की तुलना में, दोनों फेज़ चेंज मटेरियल को शामिल करने वाले द्वि-स्तरीय कैस्केड गुप्त ऊष्मा भंडारण प्रणाली चार्जिंग समय

को क्रमशः 35.23% और 10.52% तक कम करती है। कैस्केड गुप्त ऊष्मा भंडारण निकाय चार्जिंग के दौरान ऊष्मा स्थानांतरण द्रव और फेज चेंज मटेरियल्स के बीच उच्च ऊष्मा संचरण दर बनाए रखता है और विभिन्न तापमानों पर अंतिम उपयोग अनुप्रयोगों को भी सक्षम बनाता है।

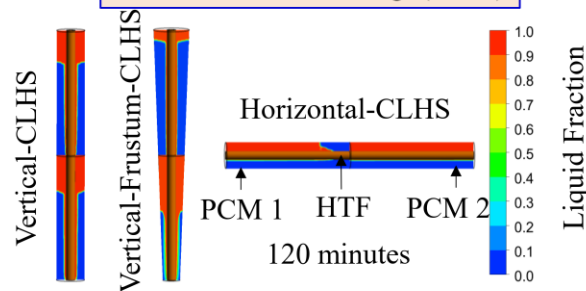
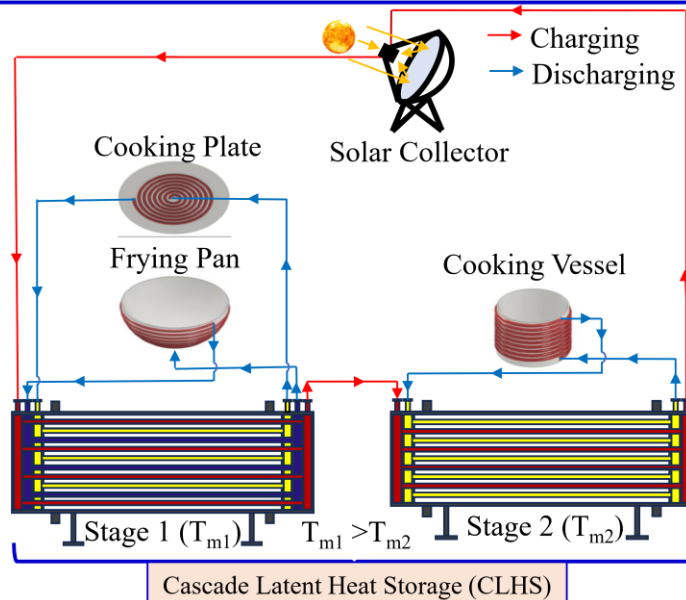
इसके अतिरिक्त, इस प्रणाली के वाणिज्यिक कार्यान्वयन के लिए सरल, निष्क्रिय, सस्ती ऊष्मा संचरण वृद्धि के तरीकों की पहचान के लिए संख्यात्मक अध्ययन किया गया है। इस अध्ययन में शेल के आकार में परिवर्तन, स्टोरेज की दिशा बदलने, और ऊष्मा स्थानांतरण द्रव मार्ग के उत्केन्द्रित विस्थापन करने के प्रभावों का विश्लेषण किया गया। बेलनाकार शेल को अर्ध-कोणीय शंकु में बदलने से चार्जिंग समय में 18.42% की कमी आती है, लेकिन यह कैस्केड गुप्त ऊष्मा भंडारण निकाय की चार्जिंग दक्षता पर नकारात्मक प्रभाव डालता है। क्षैतिज बेलनाकार कैस्केड भंडारण, अन्य भंडारण विन्यास की तुलना में, यानी एकल चरण NaNO_3 भंडारण, एकल चरण NaNO_2 भंडारण, लंबवत अर्ध-कोणीय शंकु-नुमा कैस्केड भंडारण, और लंबवत बेलनाकार कैस्केड भंडारण, क्रमशः 39.04%, 15.78%, 24.70%, और 5.9% कम चार्जिंग समय में चार्जिंग पूर्ण करता है।

संख्यात्मक अध्ययन से प्राप्त संरचना दिशानिर्देशों के आधार पर एक अत्याधुनिक और बहुपयोगी कैस्केड गुप्त ऊष्मा भंडारण निकाय विकसित किया गया है। इसके साथ ही तीन नए प्रकार के कुकिंग यूनिट - कुकिंग प्लेट, फ्राइंग पैन और कुकिंग वेसल को विकसित और इस प्रणाली में एकीकृत किया गया है, जो सेंकने, तलने और उबालने जैसे कार्यों के लिए उपयुक्त हैं। इस शोध कार्य में कैस्केड भंडारण की चक्रीय (चार्जिंग और डिस्चार्जिंग) ऊष्मीय व्यवहार और इसकी विभिन्न तापमान-आधारित अनुप्रयोगों को समर्थन करने की क्षमता का गहन विश्लेषण किया गया है। विकसित कैस्केड गुप्त ऊष्मा भंडारण निकाय सेंकने, तलने और उबालने के लिए क्रमशः कुकिंग प्लेट, फ्राइंग पैन और कुकिंग वेसल पर 473 K, 452 K और 373 K के स्थिर तापमान को बनाए रखता है। 60 ग्राम चपाती सेंकने, 80 ग्राम आलू चिप्स तलने और 500 ग्राम आलू उबालने में क्रमशः 4 मिनट, 4 मिनट और 13 मिनट लगते हैं। इस प्रणाली की चक्रीय और अंतिम उपयोग दक्षता क्रमशः 55.82% और 38.24% पाई गई। इस शोध के निष्कर्ष और सिफारिशें

कैस्केड गुप्त ऊष्मा भंडारण तकनीक के बहु-तापमान आधारित सौर तापीय और औद्योगिक अनुप्रयोगों के वाणिज्यिक उपयोग का मार्ग प्रशस्त करेंगी।

Graphical Abstract

Versatile Cascade Latent Heat Storage System for Multi-temperature Indoor Solar Cooking Applications

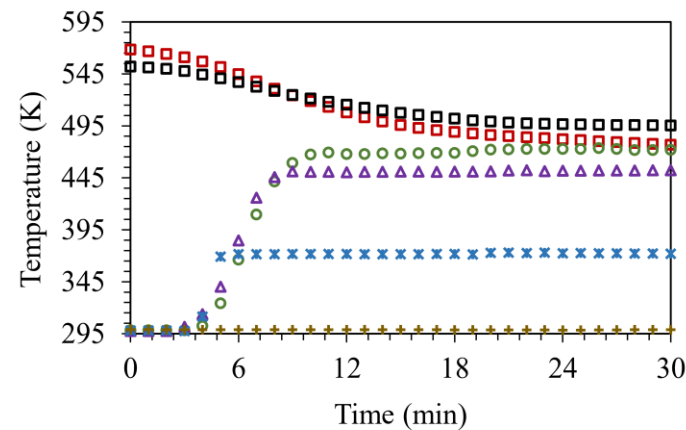


Prediction of Melting using Enthalpy Porosity Method

Advantages

- ✓ Economical and efficient energy storage system
- ✓ Fast Charging, operational simplicity, and scalable technology
- ✓ Suitable for integrating with indoor solar thermal applications
- ✓ Stable energy supply to variable temperature end-use applications with complete operation control

- PCM in Stage 1 of CLHS □ PCM in Stage 2 of CLHS
- Surface of Cooking Plate ▲ Cooking Oil in Frying Pan
- × Water in Cooking Vessel + Ambient



Temperature of CLHS and Cooking Units (Experimental Investigation)



Baking



Frying



Boiling

Contents

	Page No.
Certificate	i
Acknowledgments	ii
Abstract	iv
Graphical Abstract	xi
Contents	xii
List of Figures	xviii
List of Tables	xxv
Abbreviation	xxvi
Nomenclature	xxvii

	Page No.
Chapter 1 Introduction	1
1.1. Relevance and Justification of the Study	1
1.2. An Overview of Thermal Energy Storage Systems	7
1.2.1. Latent Heat Storage System	8
1.3. An Overview of Existing Solar Cooking Systems	11
1.3.1. Solar Cooking Using Parabolic Dish	15
1.3.2. Solar Cooking Using Scheffler Dish	15
1.3.3. Solar Cooking Using ARUN Dish	18
1.4. Concluding Remarks	19

Chapter 2 Literature Review	20
2.1. Introduction	20
2.2. Barriers to the Dissemination of Solar Cooking Technologies	20
2.3. Thermal Energy Storage for Solar Cooking Applications	28
2.4. Heat Transfer Augmentation in Latent Heat Storage Systems	33
2.4.1. Extended Surfaces/Fins	35
2.4.2. Heat Pipes	36
2.4.3. Nanoparticles	37
2.4.3. Porous Materials, Metal Matrices, and Other Low-Density Materials	40
2.4.4. Macro/Micro Encapsulation	42
2.5. Cascade Latent Heat Storage System	47
2.5.1. Numerical Investigations on Cascade Latent Heat Storage Systems	50
2.5.2. Experimental Investigations on Cascade Latent Heat Storage Systems	53
2.6. Research Gaps	57
2.7. Research Objectives	58
2.8. Outline of the Thesis	59
2.9. Concluding Remarks	63

Chapter 3	Cyclic Performance Assessment of Single and Multiple Phase Change Material-based Latent Heat Storage Systems for Medium-Temperature Applications	64
3.1.	Introduction	64
3.2.	Numerical Modelling Procedure	65
3.2.1.	Description of Physical Model	65
3.2.2.	Governing Equations and the Mathematical Formulations	68
3.2.3.	Initial and Boundary Conditions	71
3.2.4.	Assumptions Considered in the Investigation	72
3.2.5.	Numerical Procedure	73
3.2.6.	Model Validation	74
3.3.	Results and Discussion	76
3.3.1.	Performance Assessment of Storages During Charging	76
3.3.1.1.	Effect of PCM Arrangement	82
3.3.1.2.	Effect of PCM Proportion	83
3.3.1.3.	Effect of Inlet Temperature of the HTF	85
3.3.2.	Performance Assessment of Storages During Discharging	86
3.4.	Concluding Remarks	91
Chapter 4	Passive Heat Transfer Augmentation in Shell and Tube- based Latent Heat Storage System	94
4.1.	Introduction	94
4.2.	Numerical Modelling Procedure	95

4.2.1. Description of Physical Model	95
4.2.2. Governing Equations and the Mathematical Formulations	97
4.2.3. Initial and Boundary Conditions	97
4.2.4. Assumptions Considered in the Investigation	99
4.2.5. Selection of Grid Size and Time Step Size	99
4.2.6. Solution Procedure and Model Validation	101
4.3. Results and Discussion	101
4.3.1. Comparative Assessment of the Thermal Behaviour of the Vertical Cylindrical, Vertical Frustum and Horizontal Cylindrical-Latent Heat Storages	101
4.3.2. Effect of the Bottom Eccentricity of Heat Transfer Fluid Passage on Thermal Behaviour of Horizontal Cylindrical Shell and Tube-based Latent Heat Storage	109
4.4. Concluding Remarks	114
Chapter 5 Heat Transfer Augmentation in Shell and Tube-based Cascade Latent Heat Storage System	116
5.1. Introduction	116
5.2. Numerical Modelling Procedure	116
5.2.1. Description of Physical Model	116
5.2.2. Governing Equations and the Mathematical Formulations	119
5.2.3. Initial and Boundary Conditions	119

5.2.4. Assumptions Considered in the Investigation	120
5.2.5. Selection of Grid Size and Time Step Size	121
5.2.6. Solution Procedure and Model Validation	123
5.3. Results and Discussion	123
5.3.1. Comparative Assessment of Single and Multiple Phase Change Material-based Latent Heat Storage Systems	123
5.3.2. Comparative Performance Assessment of the Vertical Cylindrical and Vertical Frustum Cascade Latent Heat Storage Systems	130
5.3.3. Performance Assessment of the Vertical and Horizontal Cylindrical Cascade Latent Heat Storage Systems	133
5.3.4. Total Latent Heat Stored in Various Storage Configurations	139
5.4. Concluding Remarks	140
Chapter 6 Versatile Cascade Latent Heat Storage System for Multi- Temperature Indoor Solar Cooking Applications: Experimental Investigation and Proof of Concept	142
6.1. Introduction	142
6.2. Design and Development of the Experimental Test Facility: A Detailed Methodology	144
6.2.1. Uncertainty in the Measurements	159
6.2.2. Repeatability in the Experiments	159
6.3. Results and Discussion	161

6.3.1. Assessment of Thermal Behavior of the Cascade Latent Heat Storage System During Charging Cycle	163
6.3.2. Assessment of Thermal Behavior of the Cascade Latent Heat Storage System for Multi-temperature Cooking Applications	170
6.4. Concluding Remarks	177
Chapter 7 Conclusions and Recommendations for the Future Work	179
Appendix A: Energy Distribution in the Developed Cascade Latent Heat Storage System	183
Appendix B: Calculation of the Charging and Discharging Tubes in the Developed Cascade Latent Heat Storage System	184
Appendix C: Cost Involved in the Development of the Experimental Test Facility	187
Appendix D: Food Products Cooked Using a Developed Cooking System	189
References	190
List of Publications	217
About the Author	220

List of Figures

Figure No.	Description of Figure	Page No.
Figure 1.1	Dependency of population on polluting fuels for cooking across the world	2
Figure 1.2	Impact of using polluting fuels for cooking (an Indian perspective)	3
Figure 1.3	Charging (melting) and discharging (solidification) cycles of LHS	8
Figure 1.4	Classifications of PCMs	9
Figure 1.5	Solar cookers (a) box type cooker, (b) Panel cooker, and (c) Concentrating cooker	12
Figure 1.6	Classification of solar cooking technologies	13
Figure 1.7	Concentrating solar cookers used in cooking applications	13
Figure 1.8	Utilization of Scheffler dishes in solar cooking (a) direct solar cooking, (b) indirect solar cooking, (c) various tracking arrangements such as mechanical clock type (left) and rope motor type (right), and (d) cooking vessels	17
Figure 1.9	Comparison between market-ready solar cookers	18
Figure 2.1	Barriers to the dissemination of solar cooking technologies	27
Figure 2.2	PCMs used in solar cooking systems (% in weight)	29
Figure 2.3	Various configurations of 2-stage solar cooker	30
Figure 2.4	Various configurations of 3-stage solar cooker	31
Figure 2.5	4-stage solar cooker	32
Figure 2.6	Properties of the storage materials and their relationship with the performance of the storage	34
Figure 2.7	Heat transfer enhancement techniques for PCMs	34

Figure 2.8	Various configurations of fins used in LHES	35
Figure 2.9	Common porous materials used in LHS	42
Figure 2.10	Macro-encapsulation of PCMs	43
Figure 2.11	Layout of the arrangement of multiple PCMs in three-stage CLHS	48
Figure 2.12	Benefits of using multiple PCMs for a large operating temperature range	49
Figure 2.13	Schematic diagram of each component of the CLHS unit having molten salts as the PCMs	54
Figure 2.14	One of the two storage units of the twin, 2-stage CLHS of Peiro's experimental test facility	55
Figure 2.15	Outline of the thesis work	62
Figure 3.1	Tested storage configurations (a) single PCM-based heat storage, (b) two PCM-based cascade storage, and (c) three PCM-based cascade storage	66
Figure 3.2	Effect of various grid sizes on the melting of PCM	73
Figure 3.3	Effect of various time step sizes on the melting of PCM	74
Figure 3.4	Numerical model validation with the findings of Hosseini et al. (a) Average temperature of the PCM, (b) Local temperature in the PCM (at $r=35$ mm, $\theta=0^\circ$, $z=200$ mm)	75
Figure 3.5	Outlet temperature of the HTF during the charging cycle	77
Figure 3.6	Average liquid fraction during the charging cycle	79
Figure 3.7	Latent heat stored in various storages during a charging period of 12 h	80
Figure 3.8	Liquid fraction contours in $\text{NaNO}_3/\text{NaNO}_2$ storage at a different time of the charging process	81

Figure 3.9	Average temperature of the PCMs in NaNO ₃ /NaNO ₂ storage at different times of the charging process	82
Figure 3.10	Variation of average liquid fraction in case of the in-line and reverse arrangement of the PCMs in NaNO ₃ /NaNO ₂ storage during charging	83
Figure 3.11	Total charging time for various proportions of the PCMs in NaNO ₃ /NaNO ₂ storage	84
Figure 3.12	Total charging time of NaNO ₃ /NaNO ₂ storage for various HTF inlet conditions	85
Figure 3.13	Evolution of the outlet temperature of the HTF during the discharging process	87
Figure 3.14	Variation of average liquid fraction during the discharging process	87
Figure 3.15	Latent heat retrieved in various storage configurations during a discharge period of 12 h	88
Figure 3.16	Liquid fraction contours in KNO ₃ /NaNO ₃ storage at a different time of the discharging process	89
Figure 3.17	Average temperature of the PCMs in KNO ₃ /NaNO ₃ storage at different times of the discharging process	90
Figure 4.1	Schematics of various LHS systems	96
Figure 4.2	Applied boundary conditions	98
Figure 4.3	Computational Grid (a) Longitudinal view, (b) Cross-sectional view	99
Figure 4.4	Selection of grid size	100
Figure 4.5	Selection of time step size	100
Figure 4.6	HTF temperature at the outlet of the various storage configurations	102

Figure 4.7	Liquid fraction at different times of the charging process	103
Figure 4.8	Melting front propagation on the central axial plane in VC-LHS, VF-LHS, and HC-LHS	105
Figure 4.9	Visualization of the domain temperature on the central axial plane in VC-LHS, VF-LHS, and HC-LHS	106
Figure 4.10	Melting front propagation on the radial plane at the distance of 222 mm (top) and 666 mm (bottom) from the inlet in VC-LHS (left) and HC-LHS (right)	107
Figure 4.11	Latent thermal energy stored in the VC-LHS, VF-LHS, and HC-LHS	108
Figure 4.12	Variation of the PCM domain temperature in the HC-LHS for various bottom eccentric of HTF passage	109
Figure 4.13	Liquid fraction in the HC-LHS for various bottom eccentric locations of the HTF passage	110
Figure 4.14	Melt front movement at a radial plane located at 666 mm from the inlet in the HC-LHS for various bottom eccentric locations of the HTF passage	112
Figure 4.15	Flow pattern at a radial plane located 222 mm from the inlet in the HC-LHS for downward eccentric locations of (a) 0 mm, (b) 5 mm, (c) 10 mm, (d) 15 mm, and (e) 20 mm of the HTF flow passage at 120 minutes of the charging operation	112
Figure 4.16	Total charging time of HC-LHS for various eccentric locations of the HTF passage	113
Figure 5.1	Schematic of physical models and their orientations tested in the present study	117

Figure 5.2	Pictorial representation of the applied boundary conditions	120
Figure 5.3	Generated mesh (a) Longitudinal view, (b) Cross-sectional view	121
Figure 5.4	Effect of the count of computational elements on the liquid fraction evolution in the computational domain	122
Figure 5.5	Effect of the time step size on the liquid fraction evolution in the computational domain	122
Figure 5.6	Evolution of liquid fraction in NaNO ₃ , NaNO ₂ , NaNO ₃ /NaNO ₂ storage configurations	124
Figure 5.7	Evolution of volume average temperature of PCM in NaNO ₃ , NaNO ₂ , NaNO ₃ /NaNO ₂ storage configurations	125
Figure 5.8	Variation of the difference between the PCM temperature in any stage and their respective inlet HTF temperature	127
Figure 5.9	(a) Melt front movement and (b) temperature variation in NaNO ₃ , NaNO ₂ , NaNO ₃ /NaNO ₂ storage configurations	128
Figure 5.10	Evolution of the HTF outlet temperature in NaNO ₃ , NaNO ₂ , NaNO ₃ /NaNO ₂ storage configurations	129
Figure 5.11	Liquid fraction in various stages of the VC-CLHS and VF-CLHS	130
Figure 5.12	(a) Melt front movement and (b) temperature variation in various stages of the VC-CLHS and VF-CLHS	132
Figure 5.13	Evolution of the (a) average liquid fraction (b) liquid fraction of individual PCM in the VC-CLHS and HC-CLHS	135
Figure 5.14	(a) Melt front movement and (b) temperature variation in the VC-CLHS and HC-CLHS (at a central axial plane)	137

Figure 5.15	Melt front movement at a radial plane located at a distance of 222 mm (top) and 666 mm (bottom) from the inlet in the VC-CLHS (left) and HC-CLHS (right)	138
Figure 5.16	Evolution of the volume average temperature in the various stages of the VC-CLHS and HC-CLHS	139
Figure 5.17	Latent heat stored in various storage configurations tested in the present study	140
Figure 6.1	Experimental test facility of cascade latent heat storage system integrated with cooking plate, frying pan, and cooking vessel	146
Figure 6.2	Differential scanning calorimetry curve for NaNO ₂ and solar salt	148
Figure 6.3	Methodology adopted to calculate the number of charging and discharging tubes for both stages of the CLHS	149
Figure 6.4	Design of stage 1 of CLHS (a) Location of HTF fluid passages for charging and discharging cycles and (b) Location of various thermocouples installed	151
Figure 6.5	Design of stage 2 of CLHS (a) Location of HTF fluid passages for charging and discharging cycles and (b) Location of various thermocouples installed	152
Figure 6.6	Schematics of the cooking units	154
Figure 6.7	Outdoor experimental test facility including immersion oil heater, expansion tank, and stages 1 and 2 of versatile cascade latent heat storage system	155
Figure 6.8	Indoor experimental test facility including cooking plate, frying pan, cooking vessel, and control panel	156

Figure 6.9	Repeatability test (a) Average temperature of the PCM (b) Surface temperature of the cooking vessel	160
Figure 6.10	Variation of inlet temperature of HTF, outlet temperature of HTF, and average temperature of the PCM in stage 1 and stage 2 of the CLHS during the charging cycle	164
Figure 6.11	Temporal variation of local temperature of PCM in stage 1 of the CLHS during the charging cycle	166
Figure 6.12	Temporal variation of local temperature of PCM in stage 2 of the CLHS during the charging cycle	167
Figure 6.13	Temporal variation of the liquid fraction of PCM in stage 1 of the CLHS during the charging cycle	168
Figure 6.14	Temporal variation of the liquid fraction of PCM in stage 2 of the CLHS during the charging cycle	169
Figure 6.15	Temporal variation of local temperature of PCM in stage 1 of the CLHS during the discharging cycle	172
Figure 6.16	Temporal variation of local temperature of PCM in stage 2 of the CLHS during the discharging cycle	173
Figure 6.17	Temporal variation of the liquid fraction of PCM in stage 1 of the CLHS during the discharging cycle	174
Figure 6.18	Temporal variation of the liquid fraction of PCM in stage 2 of the CLHS during the discharging cycle	175
Figure 6.19	End-use assessment of CLHS for cooking applications	176
Figure 6.20	Cooking performed on developed cooking units (a) baking, (b) frying, (c) boiling	176

List of Tables

Table No.	Description of Table	Page No.
Table 1.1	Potential entities for solar cooking in India	3
Table 1.2	Comparison between sensible, latent, and thermochemical heat storage	10
Table 2.1	Case studies on community-scale solar cooking systems installed at various locations in India	23
Table 2.2	List of commonly used nanoparticles in LHS	38
Table 2.3	Micro & Nano-encapsulation methods for PCMs	44
Table 2.4	Summary of the advantages and disadvantages of the various heat transfer augmentation methods in PCMs	46
Table 3.1	PCMs utilized in the present investigation	67
Table 3.2	Comparative assessment of the charging and discharging cycles of the CLHS	91
Table 4.1	Thermo-physical characteristics of storage medium (NaNO ₂) and HTF (Therminol 66)	97
Table 5.1	PCMs and HTF utilized in the present work (Therminol 66)	118
Table 6.1	Thermophysical properties of the materials used in the investigation	150
Table 6.2	Specifications of the various components of the experimental test facility	157

Abbreviations

BSC	Box solar cooker
CLHS	Cascade latent heat storage
CFD	Computational fluid dynamics
CSC	Concentrating solar cooker
LHS	Latent heat storage
PCM	Phase change material
PSC	Panel solar cooker
HTF	Heat transfer fluid
HC-CLHS	Horizontal Cylindrical Cascade Latent Heat Storage
HC-LHS	Horizontal Cylindrical Latent Heat Storage
NTU	Number of transfer units
SHS	Sensible Heat Storage
TES	Thermal Energy Storage
VC-CLHS	Vertical Cylindrical Cascade Latent Heat Storage
VC-LHS	Vertical Cylindrical Latent Heat Storage
VF-CLHS	Vertical Frustum Cascade Latent Heat Storage
VF-LHS	Vertical Frustum Latent Heat Storage

Nomenclature

A_{i_f}	Inner surface area of charging/discharging tubes (m ²)
A_s	Cross-sectional area of shell excluding tube area (m ²)
A_{Mushy}	Mushy constant
c_p	Specific heat capacity of PCM (kJ/kg-K)
c_{p_f}	Specific heat capacity of HTF (kJ/kg-K)
c_{p_l}	Specific heat capacity of liquid PCM (kJ/kg-K)
c_{p_s}	Specific heat capacity of solid PCM (kJ/kg-K)
C_{min}	Minimum heat capacity (kJ/K)
d_i	Inner diameter of HTF tubes (m)
d_o	Outer diameter of HTF tubes (m)
D_i	Inner diameter of Shell (m)
E	Energy stored/released (J)
h_i	Convection heat transfer coefficient (W/m ² -K)
H_t	Total Enthalpy (kJ/kg)
h_l	Latent Thermal Energy (kJ/kg)
h_s	Sensible Thermal Energy (kJ/kg)
k	Thermal Conductivity (W/m-K)
k_f	Thermal conductivity of HTF (W/m-K)
k_w	Thermal conductivity of the tube wall (W/m-K)
L	Length of the charging/discharging tubes (m)
l_{st}	Total Length of the storage (m)
m	Mass (kg)

\dot{m}_f	Mass flow rate of HTF (kg/s)
m_{PCM}	Mass of the PCM (kg)
N	Number of Charging or Discharging tubes
p	Pressure (Pa)
\dot{q}	Heat transfer rate (W)
$Q_{HTF\text{Charging}}$	Heat lost by the HTF during charging cycle (kJ)
$Q_{PCM\text{Charging}}$	Heat stored in PCMs during charging cycle (kJ)
$Q_{PCM\text{Discharging}}$	Heat lost by the PCMs during discharging (kJ)
$Q_{Cooking}$	Heat utilized in cooking units (kJ)
R_{th}	Total thermal resistance (K/W)
r_i	Inner radius of HTF tube (m)
r_o	Outer radius of HTF tube (m)
R_i	Inner radius of shell (m)
\vec{S}_M	Momentum Source Term
$t_{charge/discharge}$	Charging or discharging time (s)
T_{fi}	Inlet temperature of HTF (K)
T_{fo}	Outlet temperature of HTF (K)
T_{pcm}	Temperature of the PCM (K)
$T_{Liquidus}$	Liquidus Temperature (K)
$T_{Solidus}$	Solidus Temperature (K)
T_{itf}	Interface Temperature (K)
$T_{initial}$	Initial Temperature (K)
T_m	Melting temperature of PCM (K)

ΔT	Temperature change of HTF during charging/discharging (K)
t	Time (seconds)
U_i	Overall heat transfer coefficient (W/m ² -K)
U_{in}	Inlet velocity of HTF (m/s)
v_f	Velocity of HTF (m/s)
V_{PCM}	Volume of the PCM (kg)
\vec{V}	Velocity Vector (m/s)
z	Axial Dimensions (m)

Greek Symbols

β	Liquid Fraction
β_t	Expansion Coefficient of PCM (1/K)
ρ	Mass Density of PCM (kg/m ³)
ρ_f	Mass Density of HTF (kg/m ³)
μ	Dynamic Viscosity (Pa-s)
μ_f	Dynamic viscosity of HTF (Pa-s)
ε	Effectiveness
θ	Angular Coordinates (degree)
η_{cyclic}	Cyclic efficiency (%)
$\eta_{End-use}$	End-use efficiency (%)